AGU PUBLICATIONS

Geophysical Research Letters

RESEARCH LETTER

10.1002/2017GL073660

Key Points:
- We examined seasonal fire danger rating forecasts for Indonesia during 2015 and 2016
- Dangerously dry conditions were predicted 180 days in advance over Borneo and New Guinea and 60 days in advance over Sumatra
- Shorter lead times over Sumatra were likely due to the absence of forecasted positive Indian Ocean Dipole conditions

Supporting Information:
- Supporting Information S1

Correspondence to:
R. D. Field,
robert.field@columbia.edu

Citation:
Shawki, D., Field, R. D., Tippett, M. K., Saharjo, B. H., Albar I., Atmoko, D., & Voulgarakis, A. (2017). Long-lead prediction of the 2015 fire and haze episode in Indonesia. *Geophysical Research Letters*, *44*, 9996–10,005. https://doi.org/10.1002/2017GL073660

Received 31 MAR 2017
Accepted 9 SEP 2017
Accepted article online 13 SEP 2017
Published online 4 OCT 2017

Long-Lead Prediction of the 2015 Fire and Haze Episode in Indonesia

Dilshad Shawki[1,2], Robert D. Field[3,4], Michael K. Tippett[4,5], Bambang Hero Saharjo[6], Israr Albar[7], Dwi Atmoko[8], and Apostolos Voulgarakis[1]

[1]Department of Physics, Imperial College London, London, UK, [2]Blackett Laboratory, Imperial College London, London, UK, [3]NASA Goddard Institute for Space Studies, New York, NY, USA, [4]Department of Applied Physics and Applied Mathematics, Columbia University, New York, NY, USA, [5]Center of Excellence for Climate Change Research, Department of Meteorology, King Abdulaziz University, Jeddah, Saudi Arabia, [6]Faculty of Forestry, Bogor Agricultural University, Bogor, Indonesia, [7]Directorate General of Climate Change, Ministry of Environment and Forestry, Jakarta, Indonesia, [8]Indonesian Agency for Meteorology, Climatology and Geophysics, Jakarta, Indonesia

Abstract We conducted a case study of National Centers for Environmental Prediction Climate Forecast System version 2 seasonal model forecast performance over Indonesia in predicting the dry conditions in 2015 that led to severe fire, in comparison to the non-El Niño dry season conditions of 2016. Forecasts of the Drought Code (DC) component of Indonesia's Fire Danger Rating System were examined across the entire equatorial Asia region and for the primary burning regions within it. Our results show that early warning lead times of high observed DC in September and October 2015 varied considerably for different regions. High DC over Southern Kalimantan and Southern New Guinea were predicted with 180 day lead times, whereas Southern Sumatra had lead times of up to only 60 days, which we attribute to the absence in the forecasts of an eastward decrease in Indian Ocean sea surface temperatures. This case study provides the starting point for longer-term evaluation of seasonal fire danger rating forecasts over Indonesia.

Plain Language Summary During the 2015 El Niño, drier-than-normal conditions led to human-caused fires getting out of control over Indonesia's fire prone regions in Sumatra and Kalimantan, and on the island of New Guinea. Recent analyses have shown that the 2015 CO_2-equivalent biomass burning emissions for all of Indonesia were in between the 2013 annual fossil fuel CO_2 emissions of Japan and India. Millions of people were exposed to hazardous air quality levels for weeks, and, at its peak, a plume of pollution from the fires stretched halfway around the world at the equator. In this study, we examined how far in advance the dangerously dry conditions could have been anticipated over different fire prone regions. We used forecasts from a coupled atmosphere-ocean model to compute 180-day forecasts of a fire danger indicator used by the Indonesian government. We found that dry conditions could have been anticipated at least 60 days in advance over Sumatra, and at least 180 days in advance over Kalimantan and New Guinea. Our analysis serves as the starting point for the development of early warning systems for fire managers in Indonesia.

1. Introduction

The 2015 fire season ranked as one of the worst on record in Indonesia, behind only 1997 and alongside 1991 and 1994 (Field et al., 2016). Surface visibility was frequently reported as less than 5% of normal, and millions of people were exposed to hazardously poor air quality for 2 months (Crippa et al., 2016; Koplitz et al., 2016; Tacconi, 2016; Voiland, 2015). Direct costs from the 2015 fires were estimated at USD 16 billion (World Bank, 2015), a conservative estimate that does not include health impacts. By mid-October, a plume of carbon monoxide from the fires stretched halfway around the world at the equator in the upper troposphere (Field et al., 2016), and total greenhouse-gas-equivalent emissions from the burning were between the mean annual fossil fuel emissions of Japan and India (Huijnen et al., 2016; Stockwell et al., 2016), contributing to the 400 ppm Mauna Loa CO_2 concentration threshold being crossed (Betts et al., 2016).

These dry season fire events have happened in Sumatra since the 1960s (van Marle et al., 2017) and in Kalimantan (Indonesian Borneo) since the 1980s (Field et al., 2009; Wooster et al., 2012) with intensifying land use pressure, the most severe of which occurred under anomalously dry conditions associated primarily with El Niño. The strength of the 2015 El Niño was comparable to the very strong 1997 event (L'Heureux et al., 2017) and, like 1997 and 2006, co-occurred with positive Indian Ocean Dipole conditions, which are thought to intensify the drying effects of El Niño over western Indonesia (Koplitz et al., 2016). The bulk of the emissions are due to burning in degraded peatlands (Levine, 1999; Page et al., 2002; Parker et al., 2016). Fires lit on the surface to clear agricultural and logging debris are more likely to escape and can spread underground into the peat. There, they cannot be suppressed with conventional fire fighting and burn until the return of the monsoon, which, during the most severe drought years, can be delayed until early November (Field et al., 2016). During normal, non-drought dry seasons, fires are less likely to escape, and there is enough precipitation to prevent most of the degraded peat from drying to its point of ignition (Field & Shen, 2008). This makes the interannual relationship between precipitation and fire emissions highly nonlinear (van der Werf et al., 2008).

Operationally, the Indonesian Agency for Meteorology, Climatology and Geophysics, (BMKG, Badan Meteorologi, Klimatologi dan Geofisika) monitors dangerously dry conditions using the national Fire Danger Rating System (FDRS), alongside basic seasonal climate assessments. The FDRS is based on the Fire Weather Index System developed in Canada and has been adopted for local use in the Indonesian fire environment (de Groot et al., 2007). Over the period 1996–2012, the ability of Fire Weather Index (FWI) System components to explain interannual variability in fire activity was as strong over Indonesia as over any part of the world (Bedia et al., 2015), with correlations between seasonal burned area and Fire Weather Index exceeding 0.8 over much of western Indonesia south of the equator. We used the Drought Code (DC) component of the Indonesian FDRS, which is its simplest component, and has been adopted to identify the potential for peat burning and severe haze (Field et al., 2004). The DC is calculated each day from the previous day's DC, and the current day's surface air temperature and daily total precipitation, and is a suitable indicator of the moisture content of heavy surface fuels and peat down to a nominal depth of 18 cm (Wotton, 2009). Experimental comparisons of the Drought Code and measured peat moisture at different depths have not been conducted in Indonesia, and its utility has rather been assessed through historical comparisons of DC variability and severe haze. During the dry seasons of 1994 and 1997, severe haze from prolonged peat burning was observed to occur when the DC was greater than 350 (de Groot et al., 2007; Field et al., 2004) but not during the non-El Niño dry seasons of 1995, 1996, or 1998. We used this threshold of 350 to interpret the differences in DC between 2015 and 2016, in terms of fire activity and forecast skill. Other components of the FDRS are used in Indonesia for distinct aspects of the fire problem, namely, the Fine Fuel Moisture Code for fire starts in lighter fuels, and the Initial Spread Index as a difficulty of control measure in grasslands (de Groot et al., 2007, 2005).

Our interest was in determining how far in advance, and with how much regional detail, dangerously dry conditions in 2015 captured by the DC could have been anticipated using seasonal forecasts from a fully coupled atmosphere-ocean model. This study builds upon previous work showing a high degree of predictability using lagged sea surface temperature indices for fire activity over Kalimantan (Ceccato et al., 2010; Wooster et al., 2012) and over the whole of Indonesia as part of a global analysis (Chen et al., 2016) and a retrospective study of the 1997–2010 precipitation forecast skill over Kalimantan at a 3 month lead time using the European Centre for Medium-Range Weather Forecasts System 4 seasonal forecast model (Spessa et al., 2015). Operationally, the DC (and all FDRS components) can be forecast using the daily output from numerical weather prediction models at different lead times. The rationale for dynamical FDRS forecasts lies therefore in their potential for seamless prediction across synoptic, subseasonal, and seasonal time scales, all of which are relevant to fire management, in their ability to physically integrate the effects of climate signals such as the Asian-Australian monsoon, the El Niño–Southern Oscillation (ENSO), the Indian Ocean Dipole (IOD), and the Madden-Julian Oscillation (MJO) across these time scales, in the expected skill improvements in the underlying forecast models (Vitart et al., 2017) and in the growing adoption of the FDRS in Indonesia among user agencies.

In this study, we considered the performance of DC forecasts from a single model, the National Centers for Environmental Prediction (NCEP) Climate Forecast System version 2 (CFSv2) (Kim et al., 2012; Saha et al., 2014) using 2015 as a case study relative to the non-El Niño dry season conditions of 2016. The skill of the DC forecasts will depend strongly on the skill of the precipitation forecasts. For CFSv2, skillful seasonal prediction of precipitation at least 4 months in advance over Indonesia is possible (Zhang et al., 2016), likely related to improvements in ENSO forecasting (Barnston & Tippett, 2013) but limited by lesser skill in predicting Indian Ocean sea surface temperature (SST) conditions for CFSv2 (Zhu et al., 2015) and other models more generally

(Shi et al., 2012). Weekly precipitation over Indonesia could be predicted with lead times of up to 1 month (Li & Robertson, 2015), likely related to skill with lead times of up to 17 days in predicting MJO events (Saha et al., 2014), which is an important factor influencing the duration of fire and haze events in Indonesia via the precipitation associated with eastward moving organized convection across western Indonesia (Reid et al., 2012).

2. Methods

We calculated 6 month DC forecasts over Indonesia using temperature and precipitation forecasts from NCEP CFSv2 (Saha et al., 2014). The CFSv2 is a comprehensive global climate model with coupled atmosphere, land, ocean, and sea ice components. The CFSv2 is initialized with observation-based estimates of the state of ocean and atmosphere and then advanced in time by integrating the equations of fluid dynamics along with physics parameterizations of unresolved processes such as convection. The atmospheric component of the CFSv2 has roughly 0.94° resolution in the horizontal and 64 levels in the vertical. Four seasonal forecasts are made each day, initialized at 0, 6 12, and 18 Z with observational estimates of the state of the ocean and atmosphere from the Climate Forecast System Reanalysis (Saha et al., 2014). We computed DC forecasts for the subsequent 6 months using the forecasts of daily surface temperature and total precipitation. Each DC forecast is initialized with the observed DC value for that day using data available from the Global Fire Weather Database (Field et al., 2015) Modern-Era Retrospective Analysis for Research and Applications version 2 (MERRA2) (Gelaro et al., 2017), the successor to the original MERRA version (Rienecker et al., 2011) in Global Fire Weather Database (GFWED). MERRA2 tends to have higher land precipitation than MERRA over Southeast Asia, but these differences are minimized over the specific regions considered in our study.

Our focus was on the forecasts leading up to the severe 2015 haze, using the wet and largely fire-free dry season of 2016 for comparison. We evaluated DC forecasts over the whole of Southern Equatorial Asia (South EQAS, 10°S to 2°N, 94°E to 153°E), a region over which seasonal precipitation forecasting skill in the region is typically described (Li & Robertson, 2015; Zhang et al., 2016). The South EQAS domain is a subregion of the standard Equatorial Southeast Asia (EQAS) domain over which fire activity has previously been described in the literature (van der Werf et al., 2010) but excludes Malaysia and northern Sumatra, which have opposite rainfall seasonality due to the northward position of the Intertropical Convergence Zone (ITCZ) during the August–October burning period that we focus on. Within Indonesia, we considered the severe burning regions of Southern Sumatra, Southern Kalimantan, and Southern New Guinea (containing parts of the Papua province of Indonesia and Papua New Guinea) to determine whether the DC forecasts were informative at scales closer to the provincial and district-level regions at which fire management agencies operate. These areas are shown in Figure 1b.

We first examined DC forecasts made in May, which correspond to a 3 month lead time prior to the onset of severe burning in mid-August 2015 (Field et al., 2016) and are similar to the lead time examined in Spessa et al. (2015) for previous fire episodes over Kalimantan. To capture the uncertainty in DC forecasts, we constructed a 32-member ensemble using the forecasts initialized every 6 h between 1 and 8 May, each with time-varying initial conditions. To account for observational uncertainty in the precipitation from which the DC is calculated, we used four different DC estimates from GFWED: Climate Prediction Center (CPC) gauge-only precipitation (Chen et al., 2008), MERRA2 reanalysis, whose precipitation is constrained only indirectly by observations, MERRA2 gauge-corrected estimates, an early Integrated Multisatellite Retrievals for Global Precipitation Measurement (IMERG) estimate (Hou et al., 2014), and a final IMERG estimate which includes gauge-based corrections. We used Aqua and Terra Moderate Resolution Imaging Spectroradiometer (MODIS) active fire detections as a metric of fire activity when interpreting the evolution of the observed DC (Giglio et al., 2003). The active fire data are available at a 1 km resolution, with their main limitations being underdetection of small fires, underground peat fires, and fires obscured by thick smoke.

3. Results

Figure 1a shows the precipitation and peatland regions, and Figure 1b shows the MODIS active fires for May 2015 while still in the wet season. The Intertropical Convergence Zone (ITCZ) was positioned

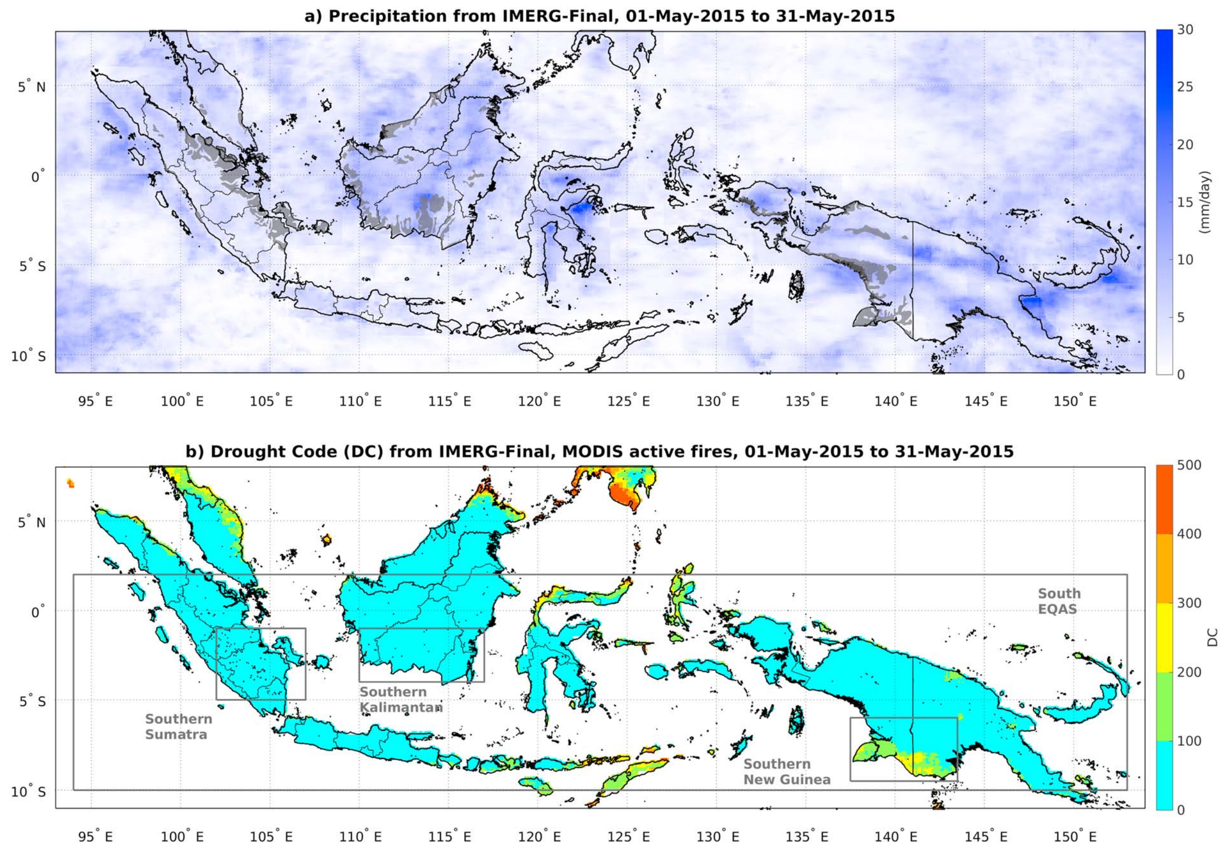

Figure 1. (a) Integrated Multisatellite Retrievals for Global Precipitation Measurement (IMERG) precipitation and peatland in grey shading and (b) Drought Code (DC) and Aqua/Terra Moderate-Resolution Imaging Spectroradiometer (MODIS) active fires as black dots over Indonesia in May 2015. The DC was calculated from daily IMERG precipitation and Modern-Era Retrospective Analysis for Research and Applications version 2 (MERRA2) surface air temperature. The grey boxes in Figure 1b define the regions over which DC forecast skill is evaluated: South Equatorial Asia (EQAS), Southern Sumatra, Southern Kalimantan, and Southern New Guinea.

directly over Indonesia at that time, leading to uniformly low (<100) DC and very little fire activity. This is in contrast to October 2015 at height of the haze event. There was a sharp north-south gradient from the area of high precipitation (Figure 2a), low DC, and little fire activity north of the equator under the ITCZ, to the area of low precipitation, high (>350) DC and extensive fire activity to the south (Figure 2b), modulated secondarily by the orography of the islands (Wooster et al., 2012; Yamanaka, 2016). The difference between May and October, and the regional variation during October, illustrates the relationship between DC and fire activity.

Figure 3 shows time series of 2015 and 2016 Aqua and Terra MODIS active fire totals, observed DC from four different estimates from GFWED, and CFSv2 DC forecasts for May initializations. In 2015 over South EQAS (Figure 3a), fire activity increased significantly in the second half of August and into September, reaching a maximum in October and dropping sharply in late October. The sharp increase in fire activity during September and October corresponded closely to the sharp increase in regional pollution from the fires (Field et al., 2016). The increase in fire was preceded by a steady DC increase across all four GFWED estimates toward above threshold (350) values in early September. Over each subregion, the DC decrease lagged behind the early November decrease in fire activity, which we interpreted as the DC capturing the moisture content of peat to a depth below which the fires are actually burning. Over all of South EQAS, the lag in DC decrease behind that in fire activity was also due to the inclusion of dry regions in the southern part of the region where severe fire is absent (i.e., Java and Nusa Tenggara) due to the absence of intensive logging, oil palm plantations, or timber plantations with which fire is strongly associated (Marlier et al., 2015) and where the monsoon returns later than to the north. In 2016, there was far less fire compared to 2015, which was reflected in the low (<200) observed DC levels. The spread in DC observations increased during dry periods, likely due to the presence of localized convective rainfall, which will be captured to varying

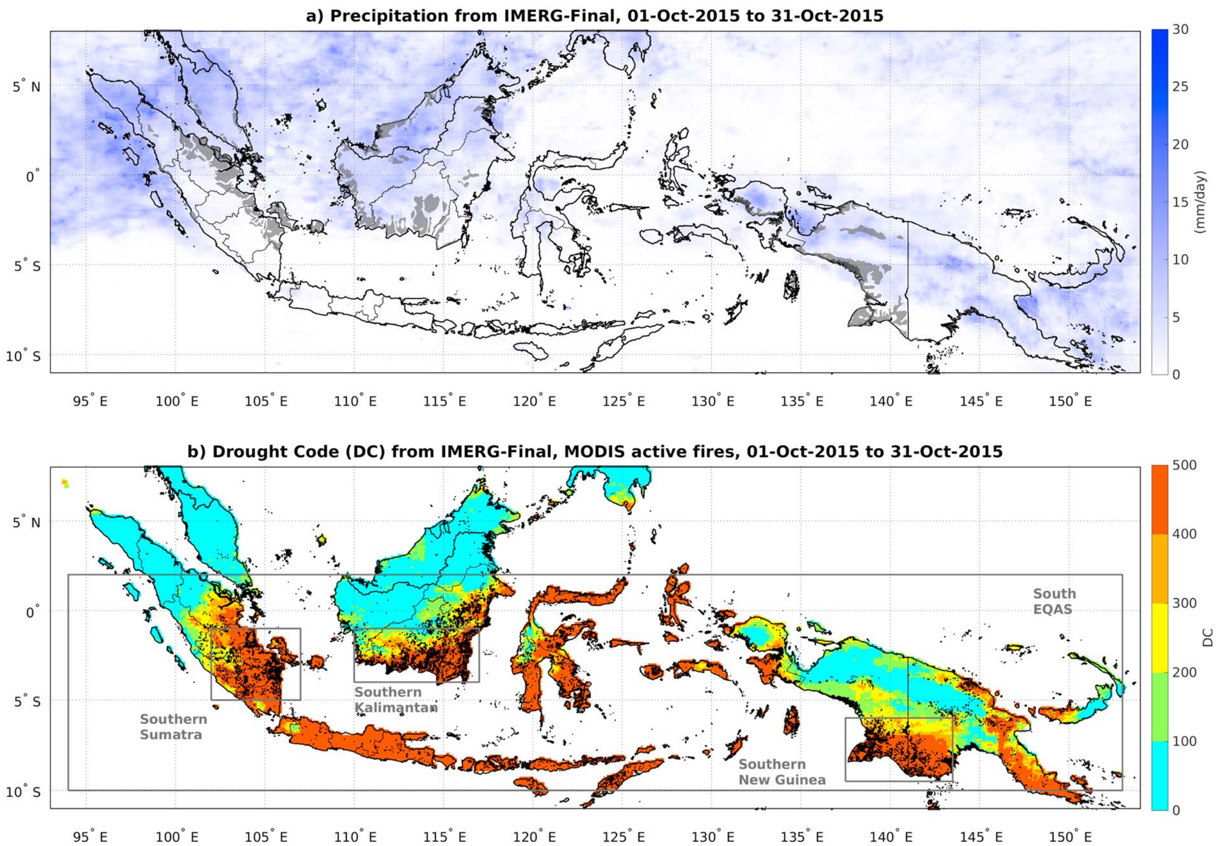

Figure 2. Same as Figure 1 but for October 2015 at the height of fire activity.

degrees by the different types of observations. For context, the maximum DC averaged from a small group of weather stations over Sumatra and Kalimantan was 500 in 1994 and 800 in 1997, both of which were severe fire years (Field et al., 2004).

Across the large South EQAS region, the May 2015 DC forecast largely captured the timing, magnitude, and decrease of the different observational estimates of DC through November. The 1σ spread of the 32-ensemble members overlapped with the spread of the different observations, except at the DC peak of ~500 in late October when, aside from the MERRA2, the upper limit of forecast DC spread (~450) fell lower than the observations. The May 2016 DC forecast peaked at ~200 compared to observed DC of 100–150, illustrating the degree to which DC forecasts for the strong El Niño of 2015 differed from those of the neutral ENSO conditions of 2016.

Within South EQAS, the May 2015 DC forecasts varied considerably in their agreement with observations. Over Southern Sumatra (Figure 3b), the May 2015 forecast was in poor agreement with observed DC, lacking the steady DC rise from August to October. This forecast missed the dangerously dry, peak DC between 450 and 600 entirely; the peak ensemble mean DC was 200, and there was no overlap between the spread in observed and forecast DC. At lead times shorter than 90 days, however, the 2015 forecast over Southern Sumatra was substantially better, which is discussed below. The May 2016 forecast was in better agreement with observed DC, showing some differentiation between El Niño and neutral ENSO conditions, but not to the degree of South EQAS as a whole.

DC over Southern Kalimantan (Figure 3c), in contrast to Southern Sumatra, was well forecast in May, with the different DC observation speaking near 500 at the end of October, and bound by the 1σ spread across ensemble members. The main limitation of the May 2015 DC forecast over Southern Kalimantan was that the predicted ensemble mean DC decrease to below threshold levels at the end of October lagged behind the observed decrease by 2 weeks. The May 2016 forecast captured the rise in DC to a peak of 200 but decreased more slowly with the onset of the monsoon than was observed.

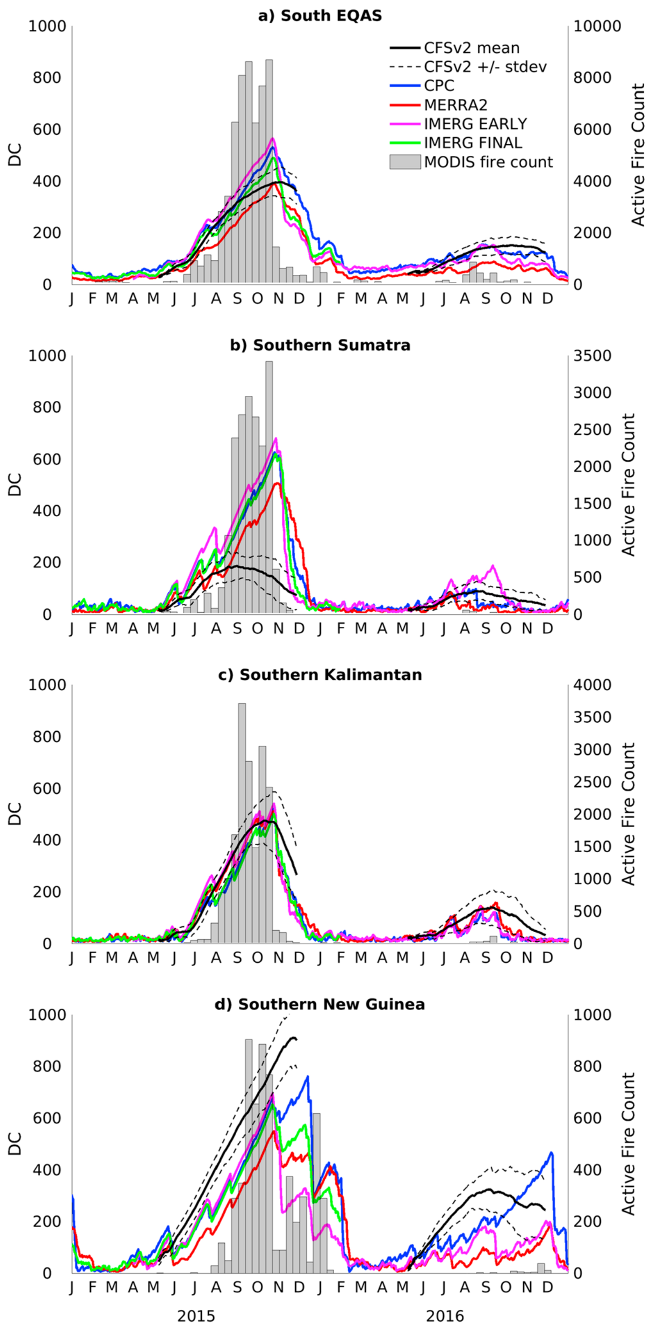

Figure 3. Time evolution of weekly MODIS active fire totals (grey bars), observed Drought Code (DC) from four Global Fire Weather Database (GFWED) estimates (colored lines) and May DC forecasts (black lines) for 180 days from NCEP CFSv2 during 2015 and 2016 over the regions identified in Figure 1: (a) South Equatorial Asia (EQAS), (b) Southern Sumatra, (c) Southern Kalimantan, and (d) Southern New Guinea. The solid black line shows the mean DC forecast across a 32-member ensemble drawn from forecasts made every 6 h between 1 and 8 May, and the dashed lines show the standard deviation across the ensemble members.

The May 2015 forecast over Southern New Guinea (Figure 3d) showed a DC increase toward above threshold values that was 6 weeks too early and peaked at 900 compared to an observed range of 550–750. The different DC observations showed steady increases through July and August, but punctuated by brief rainfall episodes which lowered the DC. These episodes were presumably absent in the forecast ensemble members, which translated into higher DC in July and August, the effect of which was carried over into September and November. Similarly, the May 2016 DC forecast was too high compared to the observations, but, like Sumatra, improves with shorter lead times and is discussed below. For both forecast years, the spread across the 32 ensemble members was larger in Southern New Guinea than in the other regions. The spread in the observations was also particularly large; the gauge-based CPC DC was significantly different than the other three versions, likely resulting from the region only having two rain gauges to represent the entire area (not shown).

To assess the DC forecasts at different lead times, Figure 4 shows every fourth (00 Z) DC forecast over each region for lead times of up to 180 days, along with the observed DC from MERRA2. Reading upward from the observed DC on the bottom row, a perfect forecast would be a continuous vertical line with the same color as the observation. These plots allowed us to determine how the DC forecast varied with lead time and identify at which lead time the forecasts captured the transition from low to high (>350) DC in early September and the termination of the event in late October/early November.

Over South EQAS as a whole (Figure 4a), the forecasts generally captured the increase to peak DC of 400 in October with up to 180 days lead time. At greater than 90 days lead time, DC between 250 and 400 was forecast for July and August compared to an observed range of 100 to 200, and there was more wavering between moderate and high DC forecast for September and October. Both of these issues lessened at lead times of less than 60 days, although at that lead time the forecasts suggested a later-than-observed drop in DC toward low wet season conditions, indicated by the rightward slanting in forecast DC after October 2015. It was only with lead times of ~20 days that transition back to low DC was forecast.

Over Southern Sumatra (Figure 4b) for lead times of greater than 90 days, there was some indication of moderately dry conditions (DC > 200) for July and August, but, as seen in the May 2015 forecast (Figure 3b), forecasts for September and October were below 100, compared to observed values approaching 500. There was a sharp transition, however, at the 60 day lead time mark. For lead times shorter than this, the DC forecasts for September and October exceeded 350 and approached 500 with 30 days lead time. The November DC decrease corresponding to the onset of the monsoon was also better forecast than for the whole of South EQAS, seen by less rightward slanting in November and December for increasing lead times. Over Southern Kalimantan (Figure 4c), like South EQAS, the high September and October DC were predicted with lead times of up to 200 days, although the forecasts consistently predicted a later decrease in DC with the onset of the monsoon than was observed in early November. In fact, the early November forecasts were better at lead times greater than 90 days, compared to shorter lead times. The forecast over

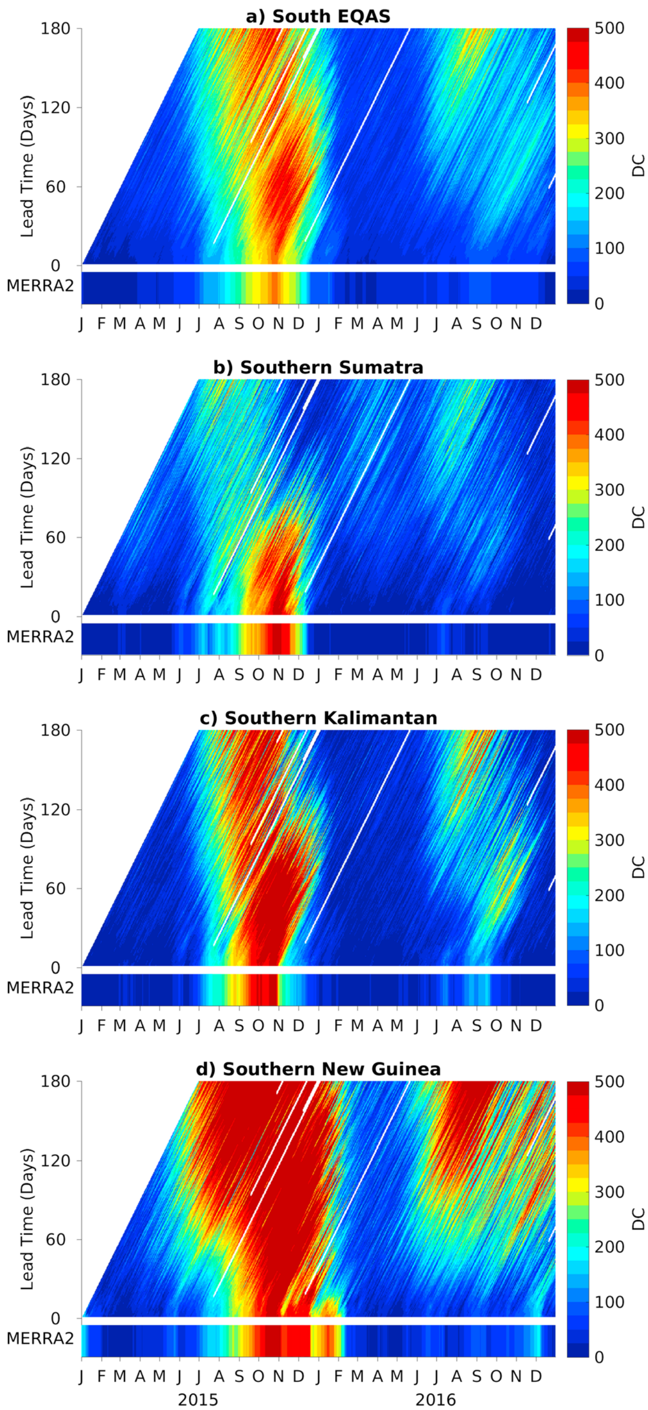

Figure 4. The 2015 and 2016 observed and forecast Drought Code (DC) for lead times of up to 180 days over (a) South Equatorial Asia (EQAS), (b) Southern Sumatra, (c) Southern Kalimantan, and (d) Southern New Guinea. In each panel, the horizontal axis is target date, and the vertical axis is lead time. The bottom strip is observed MERRA2 DC. Only forecasts initialized at 00 Z are shown. White diagonal gaps are due to sporadically missing forecast data.

Southern New Guinea (Figure 4d) persistently predicted DC exceeding 500 for June through August with lead times of greater than 60 days compared to observed values between 100 and 300 but captured the high September–November DC with lead times of up to 200 days.

The overall performance of the DC forecasts during 2015 and 2016 largely tracked that of the CFSv2 Niño 3.4 forecasts (Figure S1). In 2015, warm tropical Pacific conditions began to appear in late summer and were reasonably well forecast starting in April 2015, and the quality of the DC forecasts was also good. Forecasts of ENSO conditions made earlier in the calendar year tend to suffer from the effects of the "northern spring ENSO predictability barrier" (Barnston & Tippett, 2013; Jin et al., 2008; Tippett et al., 2012), the tendency of ENSO forecasts that cross through late spring and early summer (roughly April through June) to have relatively lower skill compared to those that do not. The skill of ENSO forecasts initialized after this period is greater, the reasons for which remain an active area of research. To varying degrees in all regions, the 2016 dry season DC forecasts were too high for lead times greater than 60–90 days. This deficiency was most pronounced over Southern New Guinea, where above threshold DC was forecast with lead times of greater than 90 days, compared to observed values less than 100. In 2016, ENSO forecasts made prior to April were especially poor, pointing toward warm conditions when in fact neutral-to-cool conditions occurred. Some of the poor performance in early 2016 may have been due to the spring predictability barrier, and, in addition, an artificial cold SST anomaly in the south equatorial Atlantic CFSv2 initial conditions that caused its ENSO forecasts in February and March 2016 to be substantially warmer than those of other models (http://www.nco.ncep.noaa.gov/pmb/changes/downloads/CFSv2_Atlantic_cold_bias_problem.pdf). These too warm ENSO forecasts were consistent with the too high DC forecasts in early 2016 at lead times of greater than 60–90 days. The CFSv2 initialization problem was remedied in the forecasts of 29 March 2016, after which CFSv2 ENSO forecasts correctly indicated cool conditions, and the corresponding forecast DC values in most regions were lower.

4. Discussion and Conclusions

For 2015 across the whole of South EQAS, the key feature of the forecasts was that the time evolution of the DC toward above threshold (>350) values in September and October values was well forecast with lead times of up to 180 days. This is consistent with previous dry season precipitation forecast skill evaluations over longer time periods, which showed strong correlations at lead times of up to 4 months (Zhang et al., 2016) over roughly the same region. For regions within Indonesia, the high DC in September and October was seen with up to 180 days lead over Southern New Guinea and Southern Kalimantan, consistent with Spessa et al.'s (2015) precipitation analysis over 1997–2010 and with a substantially lower 60 day lead time over Southern Sumatra.

In trying to understand the shorter lead times over Southern Sumatra, we note that dry season precipitation and fire activity in that region are influenced by sea surface temperature conditions over both the Pacific and

Indian Ocean basins (Abram et al., 2003; Thompson et al., 2001) to a greater degree than Kalimantan (Field et al., 2009) and, presumably, New Guinea, which are farther from the Indian Ocean. Thus, we suggest that the ability to forecast DC over Sumatra likely depended more on the model's ability to predict SST evolution in the both the Indian and Pacific Oceans, rather than mainly the Pacific. Through August–October, there was an observed eastward decrease in SSTs over the Indian Ocean associated with positive IOD conditions indicated by strongly positive Dipole Mode Index (DMI) values and cool SST anomalies off of the southwestern coast of Sumatra in September (Figure S2), which would be associated with reduced precipitation over southern Sumatra. Our preliminary examination of the CFSv2 May 2015 SST forecasts suggests that indeed, the shorter DC lead times over Sumatra were due to the absence of either or both of the eastward gradient or cool SST anomalies off of the southwestern coast of Sumatra, as indicated by only weakly positive DMI values in the May 2015 forecasts for each of August–October, which would be consistent with lower skill in CFSv2 forecasts for Indian Ocean SSTs (Zhu et al., 2015).

That said, El Niño forecasts such as that shown in Figure S1 in the supporting information will undoubtedly be the starting point for any fire and haze early warning system over Indonesia. This case study comparing 2015/2016 DC forecasts provides the starting point for the development of seasonal fire danger forecasts for fire prone regions within the country closer to the more local levels at which fire management decisions are made, using predictions from a coupled atmosphere-ocean model. The development of such systems will ideally alongside continual improvements to the FDRS in the form of field verification of its different components. The credibility of such systems will be judged on an accurate description of their limitations. The onset of high DC in Figure 4 was consistent with BMKG's precipitation forecasts at 1 month lead times (http://www.bmkg.go.id/iklim/prakiraan-hujan-bulanan.bmkg). Longer-term characterizations of FDRS forecast skill are necessary to quantify the skill and biases of seasonal fire danger forecasts and their dependence on the underlying skill of SST forecasts over both the Pacific and Indian Oceans and to understand, for example, whether the differences in seasonal forecast skill between Sumatra, Kalimantan, and New Guinea for 2015 are typical of previous years with low dry season rainfall. This would ideally be done with multiple forecast models, whose ensemble mean typically has better skill than any single model alone (Robertson et al., 2004) and provide improved uncertainty estimates (Tippett et al., 2012). Moreover, the initialization problems with CFSv2 in 2016 highlight the value of multimodel approach in operational settings.

These forecasts are useful only if used to trigger prevention and prepreparedness measures. The regulatory framework and guidance for these measures is becoming better defined, consisting of private sector equipment, detection, prevention, and training requirements, although based on audits in 2014 at least, the extent to which these requirements are being met, and their connections to early warning and detection is unclear (Saharjo & Yungan, 2017). The growing adoption of Indonesia's FDRS among user agencies has established a basic understanding of the dry conditions under which fires occur. A seasonal FDRS forecasting approach will help to spur prepreparedness and prevention activities; broadly disseminated seasonal FDRS forecasts can serve as a starting point for more compliance monitoring at the start of each dry season when dangerously dry conditions are expected and, for example, increased or reallocated resources of Ministry of Environment and Forestry "Manggala Agni" Fire Brigades which reflect regional differences in the forecasts.

Acknowledgments
All data used in the analysis can be obtained by contacting the corresponding author or from the NASA Center for Climate Simulation (ftp.nccs.nasa.gov, user: GlobalFWI, no password). R. F. was supported by the NASA Precipitation Measurement Missions Science Team and the NASA Modeling and Analysis Program. D. S. and A. V. wish to thank the European Commission's Marie Curie Actions International Research Staff Exchange Scheme (IRSES) for funding D. S.'s placement at NASA GISS and Columbia University (grant PIRSES-GA-2013-612671) and the Grantham Institute for Climate Change and the Environment for ongoing financial support. M. K. T. was partially supported by the Office of Naval Research (N00014-12-1-0911 and N00014-16-1-2073) and by NOAA's Climate Program Office's Modeling, Analysis, Predictions, and Projections program award NA14OAR4310184.

References

Abram, N. J., Gagan, M. K., McCulloch, M. T., Chappell, J., & Hantoro, W. S. (2003). Coral reef death during the 1997 Indian Ocean Dipole linked to Indonesian wildfires. *Science*, *301*(5,635), 952–955. https://doi.org/10.1126/science.1083841

Barnston, A. G., & Tippett, M. K. (2013). Predictions of Nino3.4 SST in CFSv1 and CFSv2: A diagnostic comparison. *Climate Dynamics*, *41*(5–6), 1615–1633. https://doi.org/10.1007/s00382-013-1845-2

Bedia, J., Herrera, S., Gutiérrez, J. M., Benali, A., Brands, S., Mota, B., & Moreno, J. M. (2015). Global patterns in the sensitivity of burned area to fire-weather: Implications for climate change. *Agricultural and Forest Meteorology*, *214*, 369–379.

Betts, R. A., Jones, C. D., Knight, J. R., Keeling, R. F., & Kennedy, J. J. (2016). El Niño and a record CO_2 rise. *Nature Climate Change*, *6*, 806–810. https://doi.org/10.1038/nclimate3063

Ceccato, P., Nengah Surati Jaya, I., Qian, J. H., Tippett, M. K., Robertson, A. W., & Someshwar, S. (2010). Early warning and response to fires in Kalimantan, Indonesia (Rep., p. 23).

Chen, M. Y., Shi, W., Xie, P. P., Silva, V. B. S., Kousky, V. E., Higgins, R. W., & Janowiak, J. E. (2008). Assessing objective techniques for gauge-based analyses of global daily precipitation. *Journal of Geophysical Research*, *113*, D04110. https://doi.org/10.1029/2007JD009132

Chen, Y., Morton, D. C., Andela, N., Giglio, L., & Randerson, J. T. (2016). How much global burned area can be forecast on seasonal time scales using sea surface temperatures? *Environmental Research Letters*, *11*(4), 045001. https://doi.org/10.1088/1748-9326/11/4/045001

Crippa, P., Castruccio, S., Archer-Nicholls, S., Lebron, G., Kuwata, M., Thota, A., … Spracklen, D. (2016). Population exposure to hazardous air quality due to the 2015 fires in equatorial Asia. *Scientific Reports*, *6*, 37074. https://doi.org/10.1038/srep37074

de Groot, W. J., Field, R. D., Brady, M. A., Roswintiarti, O., & Mohamad, M. (2007). Development of the Indonesian and Malaysian Fire Danger Rating Systems. *Mitigation and Adaptation Strategies for Global Change*, *12*, 165–180.
de Groot, W. J., Wardati, & Wang, Y. H. (2005). Calibrating the fine fuel moisture code for grass ignition potential in Sumatra, Indonesia. *International Journal of Wildland Fire*, *14*(2), 161–168. https://doi.org/10.1071/wf04054
Field, R. D., & Shen, S. S. P. (2008). Predictability of carbon emissions from biomass burning in Indonesia from 1997 to 2006. *Journal of Geophysical Research*, *113*, G04024. https://doi.org/10.1029/2008JG000694
Field, R. D., Spessa, A. C., Aziz, N. A., Camia, A., Cantin, A., Carr, R., … Wang, X. (2015). Development of a Global Fire Weather Database. *Natural Hazards and Earth System Sciences*, *15*(6), 1407–1423. https://doi.org/10.5194/nhess-15-1407-2015
Field, R. D., van der Werf, G. R., Fanin, T., Fetzer, E. J., Fuller, R., … Worden, H. M. (2016). Indonesian fire activity and smoke pollution in 2015 show persistent nonlinear sensitivity to El Niño-induced drought. *Proceedings of the National Academy of Sciences of the United States of America*, *113*(33), 9204–9209. https://doi.org/10.1073/pnas.1524888113
Field, R. D., van der Werf, G. R., & Shen, S. S. P. (2009). Human amplification of drought-induced biomass burning in Indonesia since 1960. *Nature Geoscience*, *2*(3), 185–188. https://doi.org/10.1038/ngeo443
Field, R. D., Wang, Y., Roswintiarti, O., & Guswanto (2004). A drought-based predictor of recent haze events in western Indonesia. *Atmospheric Environment*, *38*(13), 1869–1878. https://doi.org/10.1016/j.atmosenv.2004.01.011
Gelaro, R., McCarty, W., Suárez, M. J., Todling, R., Molod, A., Takacs, L., … Zhao, B. (2017). The Modern-Era Retrospective Analysis for Research and Applications, Version 2 (MERRA-2). *Journal of Climate*, *30*, 5419–5454. https://doi.org/10.1175/JCLI-D-16-0758.1
Giglio, L., Descloitres, J., Justice, C. O., & Kaufman, Y. J. (2003). An enhanced contextual fire detection algorithm for MODIS. *Remote Sensing of Environment*, *87*(2–3), 273–282. https://doi.org/10.1016/s0034-4257(03)00184-6
L'Heureux, M. L., Takahashi, K., Watkins, A. B., Barnston, A. G., Becker, E. J., Di Liberto, T. E., … Wittenberg, A. T. (2017). Observing and predicting the 2015/16 El Niño. *Bulletin of the American Meteorological Society*. https://doi.org/10.1175/BAMS-D-16-0009.1
Hou, A. Y., Kakar, R. K., Neeck, S., Azarbarzin, A. A., Kummerow, C. D., Kojima, M., … Iguchi, T. (2014). The Global Precipitation Measurement Mission. *Bulletin of the American Meteorological Society*, *95*(5), 701–722. https://doi.org/10.1175/bams-d-13-00164.1
Huijnen, V., Wooster, M. J., Kaiser, J. W., Gaveau, D. L. A., Flemming, J., Parrington, M., … van Weele, M. (2016). Fire carbon emissions over maritime southeast Asia in 2015 largest since 1997. *Scientific Reports*, *6*, 26886. https://doi.org/10.1038/srep26886
Jin, E. K., Kinter, J. L. III, Wang, B., Park, C. -K., Kang, I. -S., Kirtman, B. P., … Yamagata, T. (2008). Current status of ENSO prediction skill in coupled ocean-atmosphere models. *Climate Dynamics*, *31*(6), 647–664. https://doi.org/10.1007/s00382-008-0397-3
Kim, H. -M., Webster, P. J., & Curry, J. A. (2012). Seasonal prediction skill of ECMWF System 4 and NCEP CFSv2 retrospective forecast for the Northern Hemisphere winter. *Climate Dynamics*, *39*(12), 2957–2973. https://doi.org/10.1007/s00382-012-1364-6
Koplitz, S. N., Mickley, L. J., Marlier, M. E., Buonocore, J. J., Kim, P. S., Liu, T., … Schwartz, J. (2016). Public health impacts of the severe haze in equatorial Asia in September–October 2015: Demonstration of a new framework for informing fire management strategies to reduce downwind smoke exposure. *Environmental Research Letters*, *11*(9). https://doi.org/10.1088/1748-9326/11/9/094023
Levine, J. S. (1999). The 1997 fires in Kalimantan and Sumatra, Indonesia: Gaseous and particulate emissions. *Geophysical Research Letters*, *26*, 815–818. https://doi.org/10.1029/1999GL900067
Li, S., & Robertson, A. W. (2015). Evaluation of submonthly precipitation forecast skill from Global Ensemble Prediction Systems. *Monthly Weather Review*, *143*(7), 2871–2889. https://doi.org/10.1175/mwr-d-14-00277.1
Marlier, M. E., DeFries, R. S., Kim, P. S., Koplitz, S. N., Jacob, D. J., Mickley, L. J., & Myers, S. S. (2015). Fire emissions and regional air quality impacts from fires in oil palm, timber, and logging concessions in Indonesia. *Environmental Research Letters*, *10*(8). https://doi.org/10.1088/1748-9326/10/8/085005
Page, S. E., Siegert, F., Rieley, J. O., Boehm, H. D. V., Jaya, A., & Limin, S. (2002). The amount of carbon released from peat and forest fires in Indonesia during 1997. *Nature*, *420*(6,911), 61–65. https://doi.org/10.1038/nature01131
Parker, R. J., Boesch, H., Wooster, M. J., Moore, D. P., Webb, A. J., Gaveau, D., & Murdiyarso, D. (2016). Atmospheric CH_4 and CO_2 enhancements and biomass burning emission ratios derived from satellite observations of the 2015 Indonesian fire plumes. *Atmospheric Chemistry and Physics*, *16*(15), 10,111–10,131. https://doi.org/10.5194/acp-16-10111-2016
Reid, J. S., Xian, P., Hyer, E. J., Flatau, M. K., Ramirez, E. M., Turk, F. J., … Maloney, E. D. (2012). Multi-scale meteorological conceptual analysis of observed active fire hotspot activity and smoke optical depth in the Maritime Continent. *Atmospheric Chemistry and Physics*, *12*(4), 2117–2147. https://doi.org/10.5194/acp-12-2117-2012
Rienecker, M. M., Suarez, M. J., Gelaro, R., Todling, R., Bacmeister, J., Liu, E., … Woollen, J. (2011). MERRA: NASA's Modern-Era Retrospective Analysis for Research and Applications. *Journal of Climate*, *24*(14), 3624–3648. https://doi.org/10.1175/jcli-d-11-00015.1
Robertson, A. W., Lall, U., Zebiak, S. E., & Goddard, L. (2004). Improved combination of multiple atmospheric GCM ensembles for seasonal prediction. *Monthly Weather Review*, *132*(12), 2732–2744. https://doi.org/10.1175/mwr2818.1
Saha, S., Moorthi, S., Wu, X., Wang, J., Nadiga, S., Tripp, P., … Becker, E. (2014). The NCEP Climate Forecast System Version 2. *Journal of Climate*, *27*(6), 2185–2208. https://doi.org/10.1175/jcli-d-12-00823.1
Saharjo, B. H., & Yunga, A. (2017). Forest and Land Fire in Riau Province Concessions: A Case Study in Fire Prevention Policy Implementation with Local Concession Holders. In K. P. Vadrevu, T. Ohara, & C. Justice (Eds.), *Land-Atmospheric Research Applications in South and Southeast Asia* (30 pp.). Berlin: Springer, in press.
Shi, L., Hendon, H. H., Alves, O., Luo, J. J., Balmaseda, M., & Anderson, D. (2012). How predictable is the Indian Ocean Dipole? *Monthly Weather Review*, *140*(12), 3867–3884. https://doi.org/10.1175/mwr-d-12-00001.1
Spessa, A. C., Field, R. D., Pappenberger, F., Langner, A., Englhart, S., Weber, U., … Moore, J. (2015). Seasonal forecasting of fire over Kalimantan, Indonesia. *Natural Hazards and Earth System Sciences*, *15*(3), 429–442. https://doi.org/10.5194/nhess-15-429-2015
Stockwell, C. E., Jayarathne, T., Cochrane, M. A., Ryan, K. C., Putra, E. I., … Simpson, I. J. (2016). Field measurements of trace gases and aerosols emitted by peat fires in Central Kalimantan, Indonesia, during the 2015 El Niño. *Atmospheric Chemistry and Physics*, *16*(18), 11,711–11,732.
Tacconi, L. (2016). COMMENTARY: Preventing fires and haze in Southeast Asia. *Nature Climate Change*, *6*(7), 640–643.
Thompson, A. M., Witte, J. C., Hudson, R. D., Guo, H., Herman, J. R., & Fujiwara, M. (2001). Tropical tropospheric ozone and biomass burning. *Science*, *291*(5,511), 2128–2132. https://doi.org/10.1126/science.291.5511.2128
Tippett, M. K., Barnston, A. G., & Li, S. H. (2012). Performance of recent multimodel ENSO forecasts. *Journal of Applied Meteorology and Climatology*, *51*(3), 637–654. https://doi.org/10.1175/jamc-d-11-093.1
van der Werf, G. R., Dempewolf, J., Trigg, S. N., Randerson, J. T., Kasibhatla, P. S., Giglio, L., … DeFries, R. (2008). Climate regulation of fire emissions and deforestation in equatorial Asia. *Proceedings of the National Academy of Sciences of the United States of America*, *105*(51), 20,350–20,355. https://doi.org/10.1073/pnas.0803375105

van der Werf, G. R., Randerson, J. T., Giglio, L., Collatz, G. J., Mu, M., Kasibhatla, P. S., … van Leeuwen, T. T. (2010). Global fire emissions and the contribution of deforestation, savanna, forest, agricultural, and peat fires (1997–2009). *Atmospheric Chemistry and Physics*, *10*, 11,707–11,735. https://doi.org/10.5194/acp-10-11707-2010

van Marle, M. J. E., Kloster, S., Magi, B. I., Marlon, J. R., Daniau, A. -L., Field, R. D., … van der Werf, G. R. (2017). Historic global biomass burning emissions for CMIP6 (BB4CMIP) based on merging satellite observations with proxies and fire models (1750–2015). *Geoscientifc Model Development Discussions*, *10*, 3329–3357. https://doi.org/10.5194/gmd-10-3329-2017

Vitart, F., Ardilouze, C., Bonet, A., Brookshaw, A., Chen, M., Codorean, C., … Zhang, L. (2017). The subseasonal to seasonal (S2s) prediction project database. *Bulletin of the American Meteorological Society*, *98*(1), 163. https://doi.org/10.1175/bams-d-16-0017.1

Voiland, A. (2015). *Seeing Through the Smoky Pall: Observations From a Grim Indonesian Fire Season*. Greenbelt, MD: NASA Earth Observatory. https://earthobservatory.nasa.gov/Features/IndonesianFires/

Wooster, M. J., Perry, G. L. W., & Zoumas, A. (2012). Fire, drought and El Niño relationships on Borneo (Southeast Asia) in the pre-MODIS era (1980–2000). *Biogeosciences*, *9*(1), 317–340. https://doi.org/10.5194/bg-9-317-2012

World Bank (2015). Indonesia's fire crisis: Who benefits and who pays? (Rep., pp. 18–25). Jakarta, Indonesia: World Bank Group.

Wotton, B. M. (2009). Interpreting and using outputs from the Canadian Forest Fire Danger Rating System in research applications. *Environmental and Ecological Statistics*, *16*(2), 107–131. https://doi.org/10.1007/s10651-007-0084-2

Yamanaka, M. D. (2016). Physical climatology of Indonesian maritime continent: An outline to comprehend observational studies. *Atmospheric Research*, *178*, 231–259. https://doi.org/10.1016/j.atmosres.2016.03.017

Zhang, T., Yang, S., Jiang, X., & Zhao, P. (2016). Seasonal–interannual variation and prediction of wet and dry season rainfall over the Maritime Continent: Roles of ENSO and monsoon circulation. *Journal of Climate*, *29*(10), 3675–3695.

Zhu, J., Huang, B., Kumar, A., & Kinter, J. L. III (2015). Seasonality in prediction skill and predictable pattern of tropical Indian Ocean SST. *Journal of Climate*, *28*, 7962–7984. https://doi.org/10.1175/JCLI-D-15-0067.1